

1 **Effects of dissolved oxygen, pH, and anions on the 2,3-dichlorophenol degradation by**  
2 **photocatalytic reaction with anodic TiO<sub>2</sub> nanotube films**

3  
4 Hai-chao Liang<sup>a</sup>, Xiang-zhong Li<sup>a,\*</sup>, Yin-hua Yang<sup>b</sup>, Gang-hong Sze<sup>b</sup>,

5 <sup>a</sup> *Department of Civil and Structural Engineering, The Hong Kong Polytechnic University, Hong*  
6 *Kong, China*

7 <sup>b</sup> *Department of Chemistry, The Hong Kong University, Hong Kong, China*

8 *\*Corresponding author. Tel.: +852 2766 6016; Fax: +852 2334 6389.*

9 *E-mail address: cexzli@polyu.edu.hk*

10  
11 **Abstract**

12 In this study, the highly-ordered TiO<sub>2</sub> nanotube (TNT) arrays on titanium sheets were prepared  
13 by an anodic oxidation method. Under UV illumination, the TNT films demonstrated the higher  
14 photocatalytic activity in terms of 2,3-dichlorophenol (2,3-DCP) degradation in aqueous solution  
15 than the conventional TiO<sub>2</sub> thin films prepared by a sol-gel method. The effects of dissolved  
16 oxygen (DO) and pH on the photocatalytic degradation of 2,3-DCP were investigated. The results  
17 showed that the role of DO in the 2,3-DCP degradation with the TNT film was significant. It was  
18 found that 2,3-DCP in alkaline solution was degraded and dechlorinated faster than that in acidic  
19 solution whereas dissolved organic carbon removal presented an opposite order in dependence of  
20 pH. In the meantime, some main intermediate products from 2,3-DCP degradation were identified  
21 by a <sup>1</sup>H-NMR technique to explore a possible degradation pathway. A major intermediate, 2-  
22 chlororesorcinol, was identified from the 2,3-DCP decomposition as a new species compared to  
23 the findings in previous reports. Photocatalytic deactivation was also evaluated in the presence of  
24 individual anions (NO<sub>3</sub><sup>-</sup>, Cl<sup>-</sup>, SO<sub>4</sub><sup>2-</sup>, and H<sub>2</sub>PO<sub>4</sub><sup>-</sup>). The inhibition degree of photocatalytic  
25 degradation of 2,3-DCP caused by these anions can be ranked from high to low as SO<sub>4</sub><sup>2-</sup> > Cl<sup>-</sup> >  
26 H<sub>2</sub>PO<sub>4</sub><sup>-</sup> > NO<sub>3</sub><sup>-</sup>. The observed inhibition effect can be attributed to the competitive adsorption and  
27 the formation of less reactive radicals during the photocatalytic reaction.

28  
29 *Keywords:* Anion; Dissolved oxygen; Photodegradation; TiO<sub>2</sub> nanotube; 2,3-Dichlorophenol

30

## 31 **1. Introduction**

32 The halogenated aromatics in aquatic bodies are mainly from industrial wastewater and  
33 chlorination process of water purification and have been known to cause severe pollution  
34 problems (Bellar et al., 1974; Kinzell et al., 1979; Ku et al., 1996). Dichlorophenols (DCP), such  
35 as 2,3-DCP, 2,4-DCP, 2,5-DCP, and 2,6-DCP, have limited degradation by most conventional  
36 biological processes due to their toxicity (Zheng et al., 2004; Ye and Shen, 2004). The  
37 photocatalysis with immobilized TiO<sub>2</sub> thin films is an alternative to using TiO<sub>2</sub> powder with ease  
38 of separating TiO<sub>2</sub> catalyst from aqueous suspension (Arabatzis et al., 2002; Gracia et al., 2004).  
39 However, this process has limited surface area with the declined efficiency of photocatalytic  
40 reaction compared to using TiO<sub>2</sub> powder in aqueous suspension. Therefore, synthesis of the TiO<sub>2</sub>  
41 films with larger surface area and a better structure is a key step for its practical application.

42 Recently TiO<sub>2</sub> nanotube films have gained great attraction due to their large surface area, good  
43 mechanical adhesion strength, and high electronic conductivity. The immobilized TiO<sub>2</sub> nanotube  
44 films can be prepared by an anodic oxidation method through direct growth on titanium metal. As  
45 a result, this not only develops a new way to engineer TiO<sub>2</sub> nanostructures, but also explores wide  
46 applications in solar energy conversion (Hahn et al., 2007), water splitting (Mor et al., 2005), gas  
47 sensors (Mor et al., 2006), and environment purification (Quan et al., 2005; Zhuang et al., 2007).  
48 Quan et al. (2005) reported that the degradation of pentachlorophenol using an anodic TiO<sub>2</sub>  
49 nanotube film with large surface area was much faster than that using a traditional TiO<sub>2</sub> thin film  
50 formed by a sol-gel method. Xie (2006) reported that an anodic TiO<sub>2</sub>/Ti nanotubular film as a  
51 photoanode exhibited a good reactivity for the photoelectrocatalytic degradation of bisphenol A in  
52 aqueous solution. However, these works were mainly focused on the aspect of material science,  
53 but the effects of key reaction conditions such as dissolved oxygen (DO), pH, and the anions  
54 commonly contained in wastewater on the photocatalytic reaction of using the TiO<sub>2</sub> nanotube  
55 films have not well been investigated.

56 It is well known that DO can act as an electron acceptor to eliminate the recombination of  
57 photogenerated electron-hole pairs and the nanotubular TiO<sub>2</sub> surface with better separation of  
58 electrons and holes allows more efficient channeling of the charge carriers into useful reduction  
59 and oxidation reactions. On the other hand, the presence of various inorganic anions such as SO<sub>4</sub><sup>2-</sup>,  
60 Cl<sup>-</sup>, H<sub>2</sub>PO<sub>4</sub><sup>-</sup>, and NO<sub>3</sub><sup>-</sup> coexisting in various industrial effluents may cause some negative effects  
61 on the photocatalytic decomposition of organic compounds (Chen et al., 1997; Hu et al., 2003).

62 These anions are likely to retard the rates of organic compound oxidation by bidding for oxidizing  
63 radicals or by blocking the active sites of the TiO<sub>2</sub> catalyst. Therefore, this study aims at  
64 evaluating the influence of DO, pH, and selected inorganic anions on the photocatalytic  
65 degradation of 2,3-DCP in aqueous solution using the anodic TiO<sub>2</sub> nanotube films under UV light  
66 irradiation.

67

## 68 **2. Experimental**

### 69 *2.1. Materials*

70 Titanium foils (140 μm thickness, 99.6% purity) were purchased from Goodfellow Cambridge  
71 Ltd. as a raw material to prepare TiO<sub>2</sub> nanotube films. 2,3-DCP chemical with analytical grade  
72 was obtained from Aldrich Chemical Company and employed as a model pollutant. Deionized  
73 distilled water (DDW) was used throughout the experiments.

74

### 75 *2.2. Anodic oxidation process*

76 A large piece of raw Ti foil was cut into small rectangle pieces of 30 mm × 10 mm each, which  
77 were ultrasonically cleaned in acetone-ethanol solution and then rinsed by DDW as the prepared  
78 Ti foil samples. The anodic oxidation process was performed in a two-electrode cell, in which the  
79 prepared Ti foil was used as the anode and a platinum foil with the same size was employed as the  
80 cathode. Both the electrodes were submerged in aqueous 0.1 M NH<sub>4</sub>F electrolyte solution with an  
81 initial pH 1.5 and were connected with a regulated DC power supply (Kikusui Electronic Corp.  
82 Japan, PAC 35-5). All anodization experiments were conducted at a constant electrical potential of  
83 25 V and lasted for 1 h. The freshly anodized TiO<sub>2</sub>/Ti foil was washed by DDW and further  
84 calcined at 500 °C for 1 h. The product TiO<sub>2</sub> nanotubular films were named “TNT” films.

85

### 86 *2.3. Experimental*

87 One piece of TNT films with an area of 3 cm<sup>2</sup> was placed in a single-compartment reactor filled  
88 with 25 mL of aqueous 2,3-DCP solution (20 mg L<sup>-1</sup>) and an 8-W medium-pressure mercury lamp  
89 with a main emission at 365 nm (Institute of Electrical Light Source, Beijing, China) was applied  
90 as an external UV light source. A distance between the lamp and the top surface of the solution is  
91 6 cm. Prior to photoreaction, the 2,3-DCP solution was magnetically stirred in the dark for 60 min  
92 in order to achieve adsorption/desorption equilibrium. The reaction systems were aerated

93 continuously with an air flow, unless otherwise mentioned. During the photoreaction, samples  
94 were collected from the solution at different intervals for analyses.

95

#### 96 *2.4. Characterization and chemical analysis*

97 The surface morphology and element composition of the anodic TNT films were first examined  
98 by the field-emission scanning electron microscopy (FESEM) and X-ray diffraction measurement  
99 (XRD, with a Bruker D8 Discover X-ray diffractometer). To investigate the surface charges of  
100 photocatalysts in aqueous solution, zeta potential measurements were carried out using a Malvern  
101 Zetasizer 3000 (Malvern, UK). TiO<sub>2</sub> nanotubes were peeled off from TNT films to obtain TNT  
102 powder and then the TNT powder was used to prepare its suspension with a concentration of 0.1 g  
103 L<sup>-1</sup> in aqueous solution and dispersed ultrasonically for 2 h. Degussa P25 was also used to prepare  
104 its suspension with the same concentration for comparison. The 2 M HCl and 2 M NaOH solutions  
105 were used to adjust pH to the desired values. As a result, the isoelectric point of the catalysts was  
106 obtained by the measurement of the zeta-potential. 2,3-DCP concentration was analyzed by HPLC  
107 (Finnigan SpectraSYSTEM P4000) consisting of a Pinnacle II C18 reverse-phase column (5 μm,  
108 4.6 mm × 250 mm) and a UV detector (UV 6000LP). The mobile phase of acetonitrile/water (v:v  
109 = 3:2) was flowed at 1.0 mL min<sup>-1</sup>. The concentration of dissolved organic carbon (DOC) was  
110 determined by a total organic carbon analyzer (Shimadzu TOC-5000A). Chloride ions released  
111 from the 2,3-DCP degradation were determined by spectrophotometry at 460 nm after the reaction  
112 with mercury thiocyanate.

113 In order to unambiguously identify the intermediate products of 2,3-DCP degradation, <sup>1</sup>H-NMR  
114 analysis, a special feature of this study versus previous contributions (D'Oliveira et al., 1993), was  
115 employed, in which 2,3-DCP solutions of 300 mg L<sup>-1</sup> were used in photocatalytic experiments and  
116 1 mL of each sample was taken in a NMR tube at different time intervals.

117

### 118 **3. Results and discussion**

119

#### 120 *3.1. Morphology and structure of TNT film*

121 The morphology of TNT film was first examined by FESEM and its image is shown in Fig. 1a.  
122 It can be seen that the TNT film has a tubular porous structure, on which TiO<sub>2</sub> nanotubes were  
123 well-aligned as uniform arrays with high density. While the inner diameter of the nanotubes was

124 about 100 nm, the tube length was about 0.31  $\mu\text{m}$  and the wall thickness was 28 nm on average.  
125 The XRD pattern of the TNT film calcined at 500  $^{\circ}\text{C}$  was analyzed and compared with that of Ti  
126 foil, as shown in Fig. 1b. The TNT film had characteristic peaks at 25.35 $^{\circ}$  (101), 27.5 $^{\circ}$  (110), 36.1 $^{\circ}$   
127 (101), 48.1 $^{\circ}$  (200), 54.3 $^{\circ}$  (211), and 69.8 $^{\circ}$  (220), respectively. According to the XRD indexation,  
128 the crystal form of TNT is a mixture of rutile and anatase phases in good agreement with previous  
129 reports (Uchikoshi et al., 2004; Eder et al., 2006). From the FESEM and XRD results, it can be  
130 confirmed that the well-aligned  $\text{TiO}_2$  nanotubular arrays well grew on the Ti substrate successfully  
131 in aqueous  $\text{NH}_4\text{F}$  electrolyte solution during such a low-voltage anodization process.

132

133 [Fig. 1]

134

### 135 3.2. Photocatalytic activity of TNT film

136

137 The photocatalytic activity of the TNT film was evaluated in terms of 2,3-DCP degradation in  
138 aqueous solution under UV illumination. A  $\text{TiO}_2$  thin film with the same size was also prepared by  
139 the sol-gel method reported by Yu et al. (2001) and was heated at the same temperature of 500  $^{\circ}\text{C}$   
140 for comparison, which had a nonporous structure and a film thickness of  $\sim 1.0 \mu\text{m}$  (not shown  
141 here). Two experiments were conducted under same experimental condition with an initial 2,3-  
142 DCP concentration of 20  $\text{mg L}^{-1}$  and initial pH 5.3. The results are presented in Fig. 2. It can  
143 clearly be observed that after 300 min reaction while the  $\text{TiO}_2$  film degraded 2,3-DCP by less than  
144 40%, the TNT film achieved the much higher removal by 93% with a factor of about 2.6 times.  
145 Such higher reaction activity of TNT film might result from several factors of larger surface area,  
146 hollow interior walls, and a nanoscale-dimensional feature. It can be understood that when  $\text{TiO}_2$   
147 semiconductor is irradiated, electrons and holes are generated, but could recombine immediately.  
148 If the electrons and holes created do not recombine rapidly, they need to be either trapped in some  
149 metal-stable states or migrate to the semiconductor surface separately. The nanotube array  
150 architecture of the TNT film with a wall thickness of 28 nm ensures that the holes are never  
151 generated far from the semiconductor–electrolyte interface because the wall thickness is much less  
152 than the minority carrier diffusion length of  $L_p \approx 100 \text{ nm}$  in  $\text{TiO}_2$  (Hamnett, 1980), thus charge  
153 carrier separation takes place efficiently. In addition, the hollow feature of nanotubes enables the  
154 electrolyte species to permeate the entire internal and external surfaces. Paulose et al. (2006)

155 suggested that this could cause the holes to reach the electrolyte surface through diffusion, which  
156 takes place on a scale of picoseconds, and finally also reduce the bulk recombination. Besides  
157 these, the tube-to-tube contact points (~5 nm) presented in Fig. 1 may become another role  
158 responsible for the higher photoactivity for TNT film due to their quantum size effect and creation  
159 of a contact network between the nanotubes. This network let the charge carrier-transfer become  
160 easier and distance-longer. This hypothesis has been confirmed by Varghese and co-workers  
161 (2003). They stated that the nanoscale geometry of the nanotubes, in particular the tube-to-tube  
162 contact points, is believed to be responsible for the outstanding hydrogen gas sensitivity (Varghese  
163 et al., 2004). On the other hand, Lubberhuizen et al. (2000) also claimed that strong scattering  
164 inside the nanoporous network leads to a long effective path-length of photons and finally to very  
165 effective light absorption. Hence, complete light absorption is achieved in nanoporous films with a  
166 thickness considerably smaller than the light absorption depth in bulk material.

167

168 [Fig. 2]

169

### 170 3.3. Effect of DO

171 The effect of DO concentration on 2,3-DCP degradation with the initial concentration of 20 mg  
172 L<sup>-1</sup> at initial pH 5.3 was investigated in two sets of experiments using the TiO<sub>2</sub> film and TNT film  
173 by purging N<sub>2</sub>, air, or O<sub>2</sub> gas, respectively and the results are shown in Fig. 3. Figure 3 shows that  
174 after 300 min reaction under UV illumination, 2,3-DCP was degraded with the TiO<sub>2</sub> film by 49%  
175 at a high DO level of 33 mg L<sup>-1</sup> (O<sub>2</sub>), by 37% at a medium level of 8.1 mg L<sup>-1</sup> (air), and by 29% at  
176 a low level of 0.3 mg L<sup>-1</sup> (N<sub>2</sub>), respectively. It is evident that for the TiO<sub>2</sub> film, increasing the DO  
177 concentration in the solution significantly increases the extent of 2,3-DCP degradation. Meanwhile,  
178 even at the very low DO concentration (N<sub>2</sub>) the reaction rate was still significant. The similar  
179 result about the photocatalytic degradation of 4-chlorobenzoic acid using a TiO<sub>2</sub> thin film in a  
180 rotating disk photocatalytic reactor was also observed (Dionysiou et al., 2002). It has been  
181 reported that when molecular oxygen is used as an electron acceptor to trap and remove electrons  
182 from the surface of the titania particles for minimizing the build-up of free electrons, the reaction  
183 of adsorbed oxygen with photo-generated electrons at the surface of the titania catalyst is  
184 relatively slow and may be the rate-controlling step in photocatalytic oxidation reactions  
185 (Gerischer and Heller, 1991). Therefore, increasing the charge transfer rate from titania to

186 molecular oxygen will increase the efficiency of photocatalysis for organic substrate photo-  
187 oxidation. If the adsorbed oxygen is in excess of the photo-generated electrons at the surface, the  
188 rate of electron transfer to molecular oxygen will be maximized. However, they are affected by the  
189 types and characteristics of titania through the efficiency of electron-hole generation,  
190 recombination, and also charge transfer reaction rates (Almquist and Biswas, 2001).

191 For the TNT film, it can be seen from Fig. 3 that, at the very low DO concentration ( $N_2$ ), the  
192 removal of 2,3-DCP was achieved by as high as 81% after 300 min reaction. The large decay of  
193 2,3-DCP should be due to the unique nanotubular structure of TNT film, which owns a better  
194 separation of electron-hole and allows more efficient channeling of the charge carriers into the  
195 photochemical reactions, in spite of the absence of electron acceptor. Furthermore, the  
196 decomposition of 2,3-DCP increases to 93% in the presence of air and rises to 95% in the presence  
197 of oxygen, respectively. Only a slight enhancement of 2% from air to  $O_2$  gas indicates that an air  
198 saturated water system can provide sufficient electron scavengers to accelerate the photocatalytic  
199 reaction using the TNT film under UV illumination.

200

201 [Fig. 3]

202

### 203 3.4. Effect of pH

204 Solution pH is one of the most important parameters that influence the photocatalytic reactions.  
205 To study the effect of pH on the photocatalytic degradation of 2,3-DCP, one set of experiments  
206 was carried out under same experimental conditions, but different initial pH in the range of 3.4-  
207 10.9. The experimental results are shown in Table 1. It is evident that at initial pH 3.4, the pseudo-  
208 first-order rate constant ( $k$ ) of 2,3-DCP degradation was only  $7 \times 10^{-3} \text{ min}^{-1}$  and the solution pH  
209 varied from 3.4 to 3.0 after 300 min UV irradiation. Instead, at initial pH 10.9 the  $k$  value reached  
210  $24 \times 10^{-3} \text{ min}^{-1}$  (3.4 times higher than that at pH 3.4) and the corresponding pH of the solution  
211 dropped from 10.9 to 7.1. The results in Table 1 demonstrated that 2,3-DCP was degraded faster at  
212 the higher pH and some acidic products were formed from the 2,3-DCP degradation.

213

214 [Table1]

215

216 In general, medium pH has a complex effect on the photodegradation rates of chlorophenols  
217 depending on different molecular structures of chlorophenols as well as the semiconductors used  
218 in the oxidation process. Several researches showed that the removal efficiency of chlorophenols  
219 decreased with increasing pH values (Ku et al., 1996; Leyva et al., 1998; Quan et al., 2007). It is  
220 suggested that TiO<sub>2</sub> surface carries a net positive charge (pH<sub>zpc</sub> 6.25) at low pH value, while the  
221 chlorophenols and intermediates are negatively charged naturally. Because of this, low pH value  
222 can facilitate the adsorption of the organic compounds and promote better photocatalytic  
223 degradation. In contrast, better removal efficiency of chlorophenols in alkaline condition has also  
224 been reported (Stafford et al., 1994; Serpone et al., 1995; Doong et al., 2001), which is consistent  
225 with our results. It is explained that the higher pH value can provide more hydroxide ions (OH<sup>-</sup>) to  
226 react with holes to form hydroxyl radicals, subsequently enhancing the degradation rate of  
227 substituted phenols. The photocatalytic transformation of chlorophenols does not involve the •OH  
228 oxidation exclusively and direct electron transfer and surface adsorption reactions also contribute  
229 the disappearance of chlorophenols in TiO<sub>2</sub> (Stafford et al., 1994). Since the effect of pH can not  
230 be generalized, Gogate and Pandit (2004) recommended that laboratory scale studies are required  
231 for establishing the optimum pH conditions unless data are available in the literatures with exactly  
232 similar operating conditions. In our case, the faster 2,3-DCP degradation occurring at the higher  
233 pH may be attributed to two reasons: (1) more hydroxyl radicals are formed in alkaline solution  
234 with more OH<sup>-</sup> ions; and (2) it is easier for 2,3-DCP to absorb UV light energy at high pH, when  
235 the functional group of phenol is dissociated to the phenate ion due to its pK<sub>a</sub> = 7.7 (Tehan et al.,  
236 2002) and the kinetic reaction constant has been found to be greater by several orders of  
237 magnitude (Langlais et al., 1991). The much higher reactivity of the dissociated compounds at the  
238 higher pH is believed to be via the attack of electrophilic species such as •OH radicals on the  
239 phenate ion, which should be faster with a greater electron density on the aromatic ring. In contrast,  
240 at low pH the undissociated species (C<sub>6</sub>H<sub>3</sub>Cl<sub>2</sub>OH) is predominant. The hydrogen atom in polar O–  
241 H bond and the electronegative chlorine atom on o-chlorophenol may form intramolecular  
242 hydrogen bonding (O–H ··· Cl) and develop a stable 5-membered ring. This hypothesis has been  
243 supported by a number of literature precedents (Brune et al., 1999; Kolla et al., 2004). By taking  
244 into account these, a possible coordination can be found in Scheme 1. In this way, there is an  
245 increase of the o-chlorophenol resonance structure in the ground electronic state and at the same  
246 time, an increase of the surroundings rigidity occurs due to formation of the chelate ring. Both



247 effects may resist the attack of •OH radicals on the protonated phenol ring at low pH condition,  
248 evidently mirroring a corresponding decrease of the 2,3-DCP degradation.

249

250 [Scheme 1]

251

252 Table 1 also illustrates the pH dependency of the dechlorination of 2,3-DCP and DOC reduction  
253 using the TNT film. Similar to its degradation, the photocatalytic dechlorination of 2,3-DCP was  
254 observed to be faster at alkaline pH than that at acidic pH (pH 10.9 > 7.8 > 5.3 > 3.4). However,  
255 DOC reduction demonstrated an opposite result on the pH dependency, in which the  
256 photocatalytic reaction at initial pH 10.9 after 300 min UV irradiation lead to a significant release  
257 of chloride by 99% , whereas the loss of DOC was only 20%. In the case of acidic pH (pH 3.4 and  
258 5.3), the dechlorination of 2,3-DCP was only 52% and 57% after 300 min, whereas the reduction  
259 of DOC reached 47% and 40%, respectively. These results indicate that acidic condition is more  
260 favorable for the 2,3-DCP mineralization (further degradation) rather than its decomposition  
261 (initial degradation). This may be mainly attributed to the formation of organic intermediates in  
262 the photocatalytic reaction. Information on the intermediate concentrations at different pH and the  
263 pathway of 2,3-DCP degradation has been studied through the <sup>1</sup>H-NMR analysis as shown in  
264 Table 2.

265 Table 2 shows the <sup>1</sup>H-NMR spectral data of residual aromatic compounds and their corresponding  
266 concentrations at 12 h irradiation time for the photodegradation of 2,3-DCP with an initial  
267 concentration of 300 mg L<sup>-1</sup> with different initial pH. It was clearly observed that the distribution of  
268 intermediates of 2,3-DCP was pH-dependent. Compound like 2-chlororesorcinol is the major  
269 intermediate from the decomposition of 2,3-DCP under three pH conditions (pH 3.4, 5.3, and 10.9).  
270 For example, the concentration of 2-chlororesorcinol at pH 10.9 reached 90 mg L<sup>-1</sup>, which was  
271 critically higher than those at pH 3.4 (12.6 mg L<sup>-1</sup>) and 5.3 (18.9 mg L<sup>-1</sup>). Furthermore, at pH 10.9  
272 the total concentration of residual compounds in the irradiated solution (including the residual 2,3-  
273 DCP and compounds 1-7) is obviously higher than those at pH 3.4 and 5.3. This accumulated  
274 amount of 2-chlororesorcinol indicated its degradation more slowly under an alkaline condition  
275 rather than that under an acidic condition, resulting in a lower DOC reduction under the alkaline  
276 condition. Furthermore, the different concentration distribution of intermediates detected at different  
277 pH values indicates that the solution media is susceptible to OH attack on the aromatic moiety.

278 Based on the organic intermediates identified by the  $^1\text{H-NMR}$  analysis, a possible pathway of  
279 2,3-DCP degradation in this reaction system can be proposed as shown in Fig. 4. The reactions  
280 may mainly involve the addition of hydroxyl radicals to the organic substrate by three approaches  
281 of (a) hydroxylation of the aromatic ring, (b) substitution of chlorine by OH, and (c) oxidation of  
282 hydroxylated hydroquinone to the corresponding quinone (Antonarakis et al., 2002). The routes (a)  
283 and (b) in Fig. 4 was based on the dechlorination process, where the  $\bullet\text{OH}$  substitution removes the  
284 chlorine in the ring, leading to form the hydroxyl derivatives (compounds **1**, **2**, and **5**). Due to the  
285 stereochemical inhibition of *ortho*-chlorosubstituents, compound **1** is the major intermediate from  
286 the 2,3-DCP decomposition under three pH conditions.

287 In general, the OH groups in the chlorophenol ring are *ortho* and *para* directing with activation,  
288 whereas Cl substituents are *ortho* and *para* directing with deactivation. When the OH radical, an  
289 electrophilic reagent, is attacking 2,3-DCP, it is expected to attack the electron rich positions and  
290 cause to generate major *para*- or *ortho*-substituted intermediates (i.e. 3-chlorocatechol, 3,4-  
291 dichlorocatechol, and 2,3-dichloroquinol). This seems to be the case of this study. Besides the  
292 *para*- or *ortho*-substituted intermediates in present paper, however, a new intermediate, 2-  
293 chlororesorcinol, with the highest concentration was observed as *meta*-substituted intermediate  
294 under three pH conditions, which is different from the previous report (D'Oliveira et al., 1993).  
295 This indicates that this ring position is attacked by  $\bullet\text{OH}$  radical preferentially. This can be  
296 attributed to the strong stereochemical inhibition of *ortho*-chlorosubstituents to  $\bullet\text{OH}$  radical attack,  
297 due to the close proximity of OH and Cl groups on the aromatic ring (Tang and Huang, 1995)  
298 and/or to the formation of intramolecular hydrogen bonding between the OH and Cl groups in the  
299 aromatic ring (mentioned above). As a result, compound corresponding to a primary OH  
300 substitution at the *meta*-position was detected.

301 In the routes (c) and (d), the detected intermediates are all rationalized as being formed by  
302 hydrogen abstraction, followed by *para*- and *ortho*-hydroxylation of the ring, respectively.  
303 Hydroxyl radicals attack preferentially the aromatic moiety due to their electrophilic character to  
304 form the hydroxylated compounds **3** and **4**. The two products are then followed to dechlorinate  
305 through the  $\bullet\text{OH}$  attack (compound **6**) and finally oxidized to corresponding quinone (compound **7**).  
306

307 [Table 2]

308 [Fig. 4]

309

### 310 3.5. Effect of anions

311 The existence of inorganic anions such as chloride, sulfate, carbonate, nitrate, and phosphate is  
312 considerably common in wastewaters and also in natural water. The importance of anions effect  
313 on the photodegradation of pollutants has been remarkably recognized due to the occurrence of the  
314 competitive adsorption, resulting in the inhibitive effect on the photoreaction of organic pollutants.  
315 In this study, the initial pH 5.3 was employed and the effect of  $\text{Cl}^-$  on the photocatalytic  
316 degradation of 2,3-DCP in the TNT/UV system was first studied by adding NaCl into the reaction  
317 solution at different concentrations of 0.005, 0.05 and 0.1 M. The results are shown in Fig. 5a. It  
318 can be seen that while the removal of 2,3-DCP without any anion was achieved by 93% after 300  
319 min UV irradiation, it was achieved by 77% only at  $[\text{Cl}^-] = 0.005 \text{ M}$ , and further down to 64% at  
320  $[\text{Cl}^-] = 0.1 \text{ M}$ . This indicates that the rate of 2,3-DCP degradation decreased with an increased  $\text{Cl}^-$   
321 concentration significantly. The observed inhibition effect is often explained by competitive  
322 adsorption (Chen et al., 1997). To understand the adsorption behavior of the TNT catalyst in  
323 aqueous solution, the  $\text{TiO}_2$  nanotubes were peeled off from the TNT films and a powdery  
324 suspension was prepared to measure its point of zero charge (pzc) in the pH range of 3.3–10.7 as  
325 shown in Fig. 6, where P25 powder with the same concentration was also used as the reference. It  
326 can be seen that the pzc of P25 and TNT samples were at pH 6.21 and 5.23, respectively. The  
327 results demonstrated that the isoelectric point of TNT catalyst was very close to the reported value  
328 of pH 5.3 (Wang et al., 2006) and lower than that of P25 powder. In fact, the photocatalytic  
329 process mainly occurs on the photocatalyst surface, but not in the bulk solution. It is suggested that  
330 the isoelectric point would greatly influence the adsorption of organic substrates and its  
331 intermediates on the surface of photocatalyst during photoreaction (Hu et al., 2001). Therefore, the  
332  $\text{TiO}_2$  nanotube surface is positively charged at  $\text{pH} < 5.2$ , and  $\text{Cl}^-$  can be easily adsorbed onto the  
333 positively charged surface of the catalyst by electrostatic attraction, leading to the competitive  
334 adsorption.

335

336 [Fig. 5]

337 [Fig. 6]

338

339 The other probability is that chloride ions can act as scavengers of positive holes ( $h^+$ ) and/or  
340 hydroxyl radical ( $\bullet OH$ ) through the following reactions:

341



344

345 Meanwhile, the dichloride radical anion  $Cl_2\bullet^-$  from the further reaction of  $Cl\bullet$  with  $Cl^-$  (Eq. 3) is  
346 reactive with organic substances and the recombination of two chloride radicals  $Cl\bullet/Cl_2\bullet^-$  (Eqs. 4  
347 and 5) (Rincón and Pulgarin, 2004) are the source of molecular chlorine, thus ending the radicals  
348 transfer.

349



353

354 Since  $Cl\bullet$  is less reactive than  $\bullet OH$ , the excess  $Cl^-$  may have the inhibition effect on the  
355 photodegradation of 2,3-DCP in aqueous solution.

356 Figure 5b shows the effects of different anions (i.e.  $Cl^-$ ,  $NO_3^-$ ,  $H_2PO_4^-$ , and  $SO_4^{2-}$ ) at the same  
357 concentration of 0.05 M. Compared to the control test in the aqueous 2,3-DCP solutions without  
358 anion, the existence of all anions reduced the 2,3-DCP degradation to a certain degree. Among  
359 them, the strongest inhibition of 2,3-DCP degradation resulted from  $SO_4^{2-}$  due to its ionic  
360 properties. At  $pH < 5.3$ , like  $Cl^-$ ,  $SO_4^{2-}$  can inhibit the photodegradation of the chlorophenol  
361 through two ways of: (1) competitive adsorption with the 2,3-DCP on the TNT film surface due to  
362 the higher ionic strength and (2) trapping positive holes and/or hydroxyl radical, where  $SO_4^{2-}$  can  
363 be led to the generation of less reactive radical  $SO_4\bullet^-$ . Actually, the divalence charge for  $SO_4^{2-}$  can  
364 lead to the stronger binding of the  $SO_4^{2-}$  with the catalyst, as compared with the single valence  
365 ions such as  $NO_3^-$ ,  $Cl^-$ , and  $H_2PO_4^-$ , thus resulting in the stronger competitive adsorption. For the  
366 addition of  $H_2PO_4^-$ , the behavior of  $H_2PO_4^-$  ions is similar to  $SO_4^{2-}$  ions, in that the  $H_2PO_4^-$   
367 reacted with  $h^+$  and  $\bullet OH$  to form  $H_2PO_4\bullet^-$ , less reactive than that of  $h^+$  and  $\bullet OH$ . Formation of  
368 inorganic radical anions under these circumstances was also reported in some literatures (Abdullah  
369 et al., 1990; Bekbölet et al., 1998; Hu et al., 2003). The addition of  $NO_3^-$  to the solution in this

370 study showed a minor effect on the photocatalytic degradation of 2,3-DCP only. Abdullah et al.  
371 (1990) also reported that the presence of  $\text{NaNO}_3$  had negligible effect on the photodegradation of  
372 ethanol and 2-propanol under UV light irradiation. On the basis of above discussion, the observed  
373 inhibition effect may be therefore explained by combination of the competitive adsorption and the  
374 formation of less reactive radicals during the photocatalytic reaction.

375

#### 376 **4. Conclusions**

377 The highly-ordered  $\text{TiO}_2$  nanotube arrays were successfully formed on Ti foil by an anodic  
378 oxidation method. The experimental results showed that the anodic TNT film had the higher  
379 photocatalytic activity than the conventional  $\text{TiO}_2$  thin film prepared by a sol-gel method with a  
380 factor of about 2.6 times. DO acts as an effective electron acceptor to extend the hole's lifetime  
381 and to form the oxidizing species of  $\bullet\text{OH}$  radicals, affecting the photoactivity of the TNT film.  
382 Effect of solution pH demonstrated that an alkaline condition is favorable to 2,3-DCP degradation  
383 and dechlorination, but an acidic condition is more beneficial to further mineralization. The  
384 presence of  $\text{NO}_3^-$  had a weak inhibition effect on the degradation of 2,3-DCP, while  $\text{SO}_4^{2-}$  had the  
385 strongest inhibition.

386

#### 387 **Acknowledgements**

388 The authors wish to acknowledge the support of the Research Committee of The Hong Kong  
389 Polytechnic University in providing a PhD scholarship for H. C. Liang.

390

#### 391 **References**

392

393 Abdullah, M., Low, K.C., Mattheus, R.W., 1990. Effects of common inorganic anions on rates of  
394 photocatalytic oxidation of organic carbon over illuminated titanium dioxide. *J. Phys. Chem.*  
395 94, 6820-6825.

396 Almquist, C.B., Biswas, P., 2001. A mechanistic approach to modeling the effect of dissolved  
397 oxygen in photo-oxidation reactions on titanium dioxide in aqueous systems. *Chem. Eng. Sci.*  
398 56, 3421-3430.

399 Antonaraki, S., Androulaki, E., Dimotikali, D., Hiskia, A., Papaconstantinou, E., 2002. Photolytic  
400 degradation of all chlorophenols with polyoxometallates and H<sub>2</sub>O<sub>2</sub>. *J. Photochem. Photobiol.*  
401 *A* 148, 191-197.

402 Arabatzis, I.M., Antonaraki, S., Stergiopoulos, T., Hiskia, A., Papaconstantinou, E., Bernard, M.C.,  
403 Falaras, P., 2002. Preparation, characterization and photocatalytic activity of nanocrystalline  
404 thin film TiO<sub>2</sub> catalysts towards 3,5-dichlorophenol degradation. *J. Photochem. Photobiol. A*  
405 149, 237-245.

406 Bekbölet, M., Boyacioglu, Z., Özkaraova, B., 1998. The influence of solution matrix on the  
407 photocatalytic removal of color from natural waters. *Water Sci. Technol.* 38(6), 155-162.

408 Bellar, J.A., Lichtenberg, J.J., Kroner, R.C., 1974. The occurrence of organohalides in chlorinated  
409 drinking waters. *J. Am. Water Works Ass.* 66(22), 703-706.

410 Brune, B.J., Koehler, J.A., Smith, P.J., Payne, G.F., 1999. Correlation between adsorption and  
411 small molecule hydrogen bonding. *Langmuir* 15, 3987-3992.

412 Chen, H.Y., Zahraa, O., Bouchy, M., 1997. Inhibition of the adsorption and photocatalytic  
413 degradation of an organic contaminant in an aqueous suspension of TiO<sub>2</sub> by inorganic ions. *J.*  
414 *Photochem. Photobiol. A* 108, 37-44.

415 Dionysiou, D.D., Burbano, A.A., Suidan, M.T., Baudin, I., Laine, J.M., 2002. Effect of oxygen in  
416 a thin-film rotating disk photocatalytic reactor. *Environ. Sci. Technol.* 36, 3834-3843.

417 D'Oliveira, J.C., Minerob, C., Pelizzetti, E., Pichat, P., 1993. Photodegradation of  
418 dichlorophenols and trichlorophenols in TiO<sub>2</sub> aqueous suspensions: kinetic effects of the  
419 positions of the Cl atoms and identification of the intermediates. *J. Photochem. Photobiol. A*  
420 72, 261-267.

421 Doong, R.A., Chen, C.H., Maithreepala, R.A., Chang, S.M., 2001. The influence of pH and  
422 cadmium sulfide on the photocatalytic degradation of 2-chlorophenol in titanium dioxide  
423 suspensions. *Water Res.* 35, 2873-2880.

424 Eder, D., Kinloch, I.A., Windle, A.H., 2006. Pure rutile nanotubes. *Chem. Commun.* 13, 1448-  
425 1450.

426 Gerischer, H., Heller, A., 1991. The role of oxygen in photooxidation of organic molecules on  
427 semiconductor particles. *J. Phys. Chem.* 95, 5261-5267.

428 Gogate, P.R., Pandit, A.B., 2004. A review of imperative technologies for wastewater treatment I:  
429 Oxidation technologies at ambient conditions. *Adv. Environ. Res.* 8, 501-551.

430 Gracia, F., Holgado, J.P., González-Elipé, A.R., 2004. Photoefficiency and optical, microstructural,  
431 and structural properties of TiO<sub>2</sub> thin films used as photoanodes. *Langmuir* 20, 1688-1697.

432 Hagfeldt, A., Grätzel, M., 1995. Light-induced redox reactions in nanocrystalline systems, *Chem.*  
433 *Rev.* 95 (1995) 49–54.

434 Hahn, R., Stergiopoulos, T., Macak, J.M., Tsoukleris, D., Kontos, A.G., Albu, S.P., Kim, D.,  
435 Ghicov, A., Kunze, J., Falaras, P., Schmuki, P., 2007. Efficient solar energy conversion using  
436 TiO<sub>2</sub> nanotubes produced by rapid breakdown anodization – A comparison. *Phys. Stat. Sol.*  
437 (RRL) 1, 135-137.

438 Hamnett, A., 1980. Porous-electrodes for water oxidation. *Faraday Discuss. Chem. Soc.* 70, 127-  
439 134.

440 Hu, C., Wang, Y.Z., Tang, H.X., 2001. Influence of adsorption on the photodegradation of various  
441 dyes using surface bond-conjugated TiO<sub>2</sub>/SiO<sub>2</sub> photocatalyst. *Appl. Catal. B-Environ.* 35, 95-  
442 105.

443 Hu, C., Yu, J.C., Hao, Z., Wong, P.K., 2003. Effects of acidity and inorganic ions on the  
444 photocatalytic degradation of different azo dyes. *Appl. Catal. B-Environ.* 46, 35-47.

445 Kinzell, L.H., McKenzie, R.M., Olson, B.A., Kirsch, D.G., Shull, L.R., 1979. Priority pollutants, I:  
446 A perspective view. *Environ. Sci. Technol.* 13, 416-423.

447 Kolla, A., Parasukb, V., Parasukc, W., Karpfend, A., Wolschann, P., 2004. Theoretical study on  
448 the intramolecular hydrogen bond in chloro-substituted N,N-dimethylaminomethylphenols. I.  
449 Structural effects. *J. Mol. Struct.* 690, 165-174.

450 Ku, Y., Leu, R.M., Lee, K.C., 1996. Decomposition of 2-chlorophenol in aqueous solution by UV  
451 irradiation with the presence of titanium dioxide. *Water Res.* 30, 2569-2578.

452 Lagemaat, J., Plakman, M., Vanmaekelbergh, D., Kelly, J.J., 1996. Enhancement of the light-to-  
453 current conversion efficiency in an n-SiC/solution diode by porous etching, *Appl. Phys. Lett.*  
454 69, 2246-2248.

455 Langlais, B., Reckhow, D.A., Brink, R.B. (Eds.), 1991. *Ozone in water treatment—Application*  
456 *and engineering.* Lewis Publishers, Chelsea, USA, pp. 43-45.

457 Leyva, E., Moctezuma, E., Ruíz, M.G., Martínez, L., 1998. Photodegradation of phenol and 4-  
458 chlorophenol by BaO–Li<sub>2</sub>O–TiO<sub>2</sub> catalysts. *Catal. Today* 40, 367-376.

459 Lubberhuizen, W.H., Vanmaekelbergh, D., Van Faassen, E., 2000. Recombination of  
460 photogenerated charge carriers in nanoporous gallium phosphide, *J. Porous Mater.* 7, 147-152.

461 Mor, G.K., Shankar, K., Paulose, M., Varghese, O.K., Grimes, C.A., 2005. Enhanced  
462 photocleavage of water using titania nanotube arrays. *Nano Lett.* 5, 191-195.

463 Mor, G.K., Varghese, O.K., Paulose, M., Ong, K.G., Grimes, C.A., 2006. Fabrication of hydrogen  
464 sensors with transparent titanium oxide nanotube-array thin films as sensing elements. *Thin*  
465 *Solid Films* 496, 42-48.

466 Paulose, M., Mor, G.K., Varghese, O.K., Shankar, K., Grimes, C.A., 2006. Visible light  
467 photoelectrochemical and water-photoelectrolysis properties of titania nanotube arrays. *J.*  
468 *Photochem. Photobiol. A* 178, 8-15.

469 Quan, X., Ruan, X.L., Zhao, H.M., Chen, S., Zhao, Y.Z., 2007. Photoelectrocatalytic degradation  
470 of pentachlorophenol in aqueous solution using a TiO<sub>2</sub> nanotube film electrode. *Environ.*  
471 *Pollut.* 147, 409-414.

472 Quan, X., Yang, S.G., Ruan, X.L., Zhao, D.M., 2005. Preparation of titania nanotubes and their  
473 environmental applications as electrode. *Environ. Sci. Technol.* 39, 3770-3775.

474 Rincón, A.G., Pulgarin, C., 2004. Effect of pH, inorganic ions, organic matter and H<sub>2</sub>O<sub>2</sub> on *E. coli*  
475 K12 photocatalytic inactivation by TiO<sub>2</sub> implications in solar water disinfection. *Appl. Catal.*  
476 *B-Environ.* 51, 283-302.

477 Serpone, N., Maruthamuthu, P., Pichat, P., Pelizzetti, E., Hidaka, H., 1995. Exploiting the  
478 interparticle electron transfer process in the photocatalyzed oxidation of phenol, 2-  
479 chlorophenol and pentachlorophenol: chemical evidence for electron and hole transfer  
480 between coupled semiconductors. *J. Photochem. Photobiol. A* 85, 247-255.

481 Stafford, U., Gray, K.A., Kamat, P.V., 1994. Radiolytic and TiO<sub>2</sub>-assisted photocatalytic  
482 degradation of 4-chlorophenol. A comparative study. *J. Phys. Chem.* 98, 6343-6351.

483 Sukanto, J.P.H., Smyrl, W.H., Mcmillan, C.S., Kozlowski, M.R., 1992. Photoelectrochemical  
484 measurements of thin oxide-films—multiple internal-reflection effects. *J. Electrochem. Soc.*  
485 139, 1033-1043.

486 Tang, W.Z., Huang, C.P., 1995. The effect of chlorine position of chlorinated phenols on their  
487 dechlorination kinetics by Fenton's reagent. *Waste Manage.* 15, 615-622.

488 Tehan, B.G., Lloyd, E.J., Wong, M.G., Pitt, W.R., Montana, J.G., Manallack, D.T., Gancia, E.,  
489 2002. Estimation of pK<sub>a</sub> using semiempirical molecular orbital methods. Part 1: Application  
490 to phenols and carboxylic acids. *Quant. Struct-Act. Rel.* 21, 457-472.



491 Uchikoshi, T., Suzuki, T.S., Tang, F., Okuyama, H., Sakka, Y., 2004. Crystalline-oriented TiO<sub>2</sub>  
492 fabricated by the electrophoretic deposition in a strong magnetic field. *Ceramic Inter.* 30,  
493 1975-1978.

494 Varghese, O.K., Gong, D., Paulose, M., Ong, K.G., Dickey, E.C., Grimes, C.A., 2003. Extreme  
495 changes in the electrical resistance of titania nanotubes with hydrogen exposure. *Adv. Mater.*  
496 15, 624-627.

497 Varghese, O.K., Mor, G.K., Grimes, C.A., Paulose, M., Mukherjeeb, N., 2004. A titania nanotube-  
498 array room-temperature sensor for selective detection of hydrogen at low concentrations. *J.*  
499 *Nanosci. Nanotechnol.* 4, 733-737.

500 Wang, N., Lin, H., Li, J.B., Yang, X.Z., Chi, B., 2006. Electrophoretic deposition and optical  
501 property of titania nanotubes films. *Thin Solid Films* 496, 649-652.

502 Xie, Y.B., 2006. Photoelectrochemical application of nanotubular titania photoanode. *Electrochim.*  
503 *Acta* 51, 3399-3406.

504 Ye, F.X., Shen, D.S., 2004. Acclimation of anaerobic sludge degrading chlorophenols and the  
505 biodegradation kinetics during acclimation period. *Chemosphere* 54, 1573-1580.

506 Yu, J.G., Zhao, X.J., Zhao, Q.N., 2001. Photocatalytic activity of nanometer TiO<sub>2</sub> thin films  
507 prepared by the sol-gel method. *Mater. Chem. Phys.* 69, 25-29.

508 Zheng, S.K., Yang, Z.F., Job, D.H., Yun Hee Park, Y.H., 2004. Removal of chlorophenols from  
509 groundwater by chitosan sorption. *Water Res.* 38, 2315-2322.

510 Zhuang, H.F., Lin, C.J., Lai, Y.K., Sun, L., Li, J., 2007. Some critical structure factors of titanium  
511 oxide nanotube array in its photocatalytic activity. *Environ. Sci. Technol.* 41, 4735-4740.

512

513

514 **List of figure captions**

515

516 Fig. 1. (a) FESEM images of TNT film; (b) XRD patterns of Ti foil and TNT film calcined at 500  
517 °C for 1 h.

518

519 Fig. 2. 2,3-DCP degradation with TiO<sub>2</sub> film and TNT film under UV illumination (Initial pH 5.3  
520 and [C<sub>0</sub>] = 20 mg L<sup>-1</sup>).

521

522 Fig. 3. Effect of DO concentration on 2,3-DCP degradation with TiO<sub>2</sub> film and TNT film by  
523 blowing different gases (N<sub>2</sub>, air or O<sub>2</sub>), respectively (Initial pH 5.3 and [C<sub>0</sub>] = 20 mg L<sup>-1</sup>).

524

525 Fig. 4. Pathway of the 2,3-DCP degradation in the TNT/UV system.

526

527 Fig. 5. (a) Influence of Cl<sup>-</sup> concentrations on the photocatalytic deactivation of TNT/UV system  
528 (Initial pH 5.3 and [C<sub>0</sub>] = 20 mg L<sup>-1</sup>); (b) Photocatalytic deactivation in the presence of  
529 different anions at 0.05 M (Initial pH 5.3 and [C<sub>0</sub>] = 20 mg L<sup>-1</sup>): (●) no anion; (■) NO<sub>3</sub><sup>-</sup>; (▲)  
530 H<sub>2</sub>PO<sub>4</sub><sup>-</sup>; (▼) Cl<sup>-</sup>; (◆) SO<sub>4</sub><sup>2-</sup>.

531

532 Fig. 6. Zeta potential analysis of P25 and TNT samples as a function of pH.

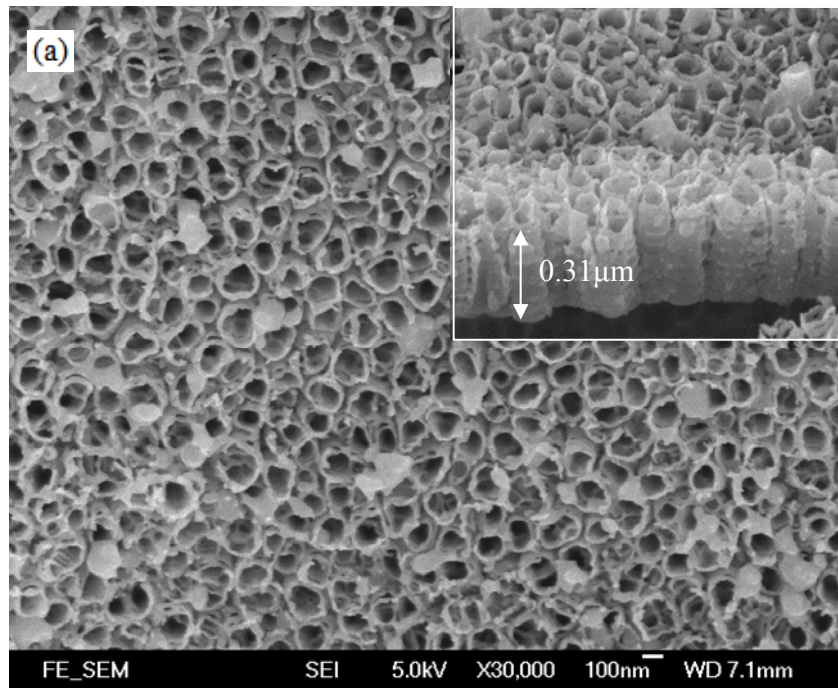
533

534 Scheme 1. Formation of intramolecular hydrogen bonding in 2,3-DCP molecular structure.

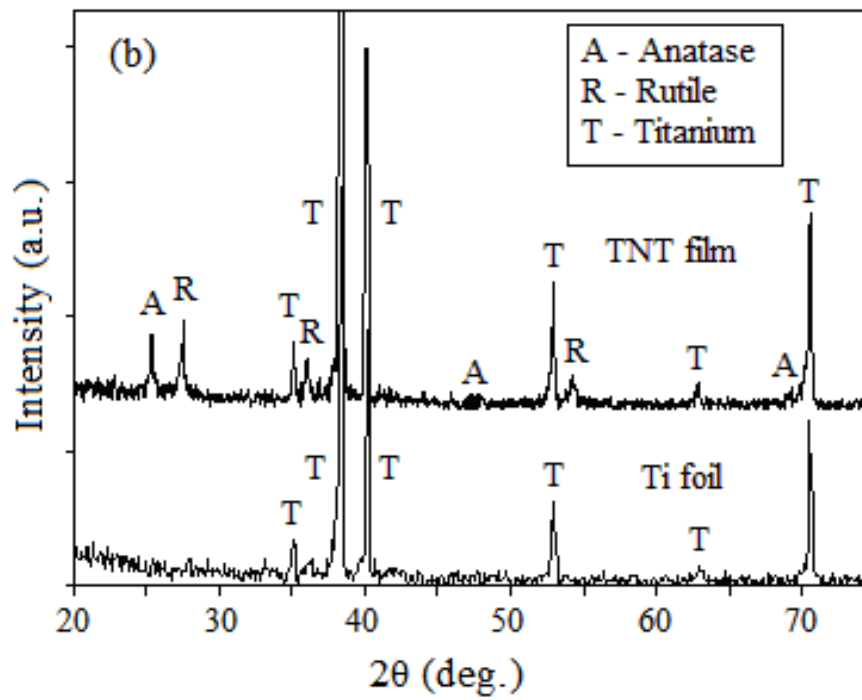
535

536

537 Fig. 1.



538



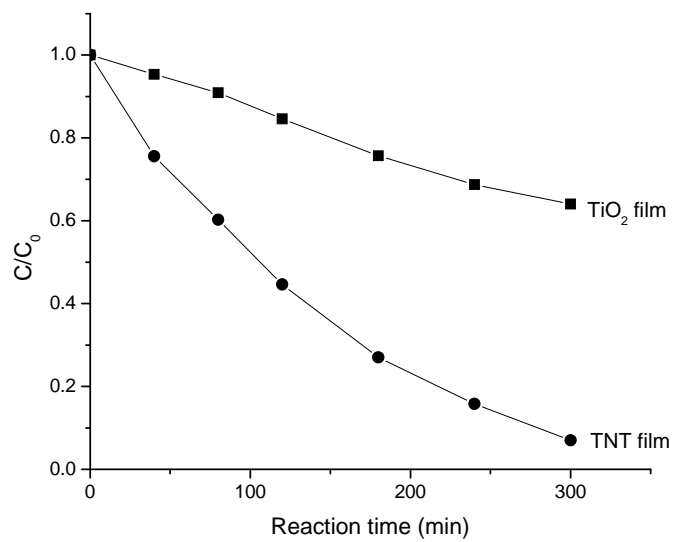
539

540

541

542 Fig. 2

543



544

545

546

547

548

549

550

551

552

553

554

555

556

557

558

559

560

561

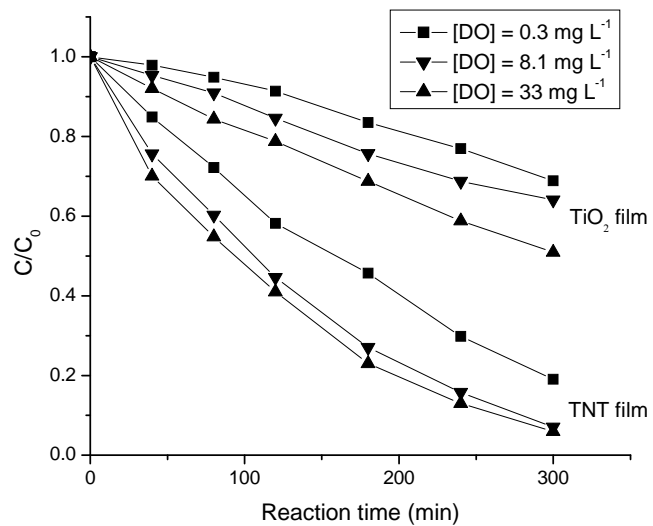
562

563

564 Fig. 3

565

566



567

568

569

570

571

572

573

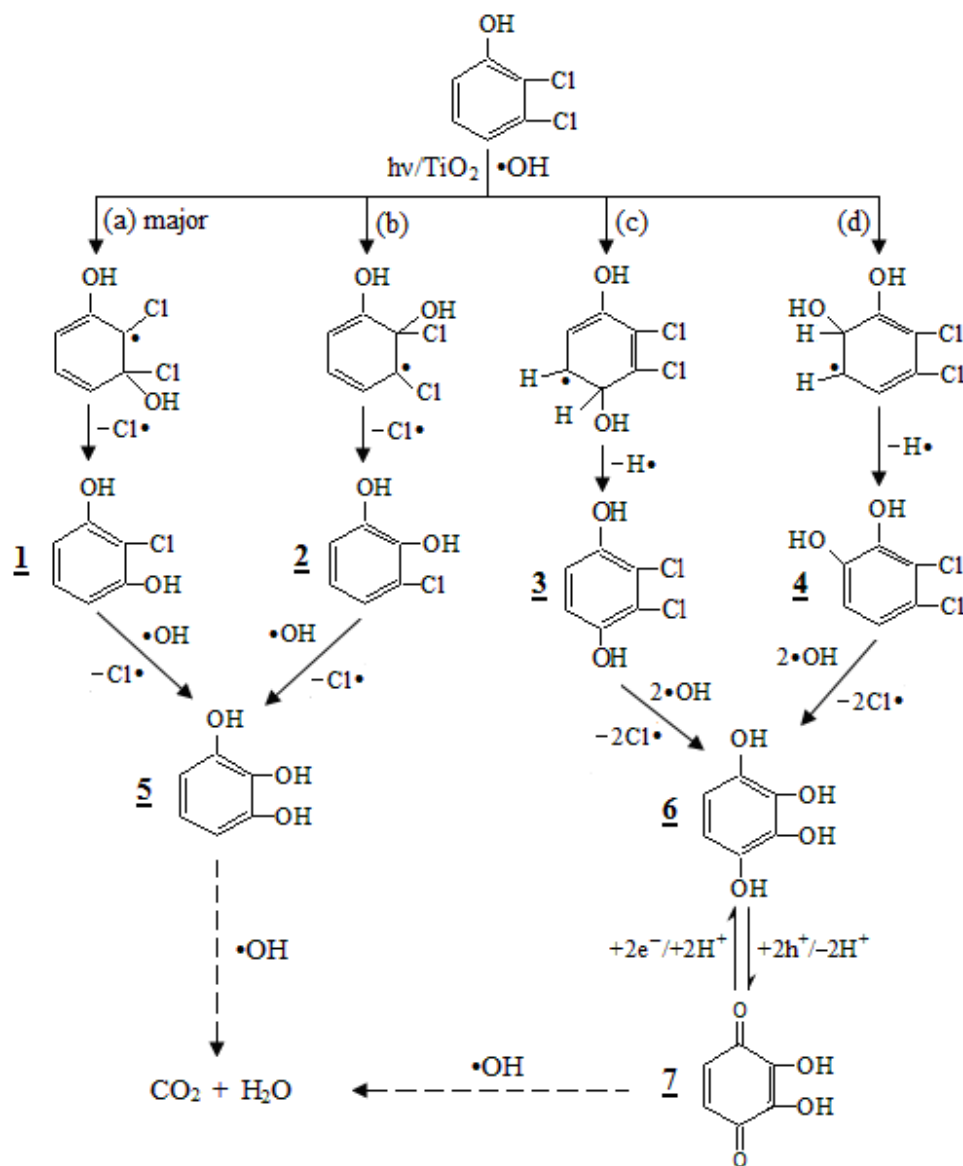
574

575

576 Fig. 4

577

578



579

580

581

582

583

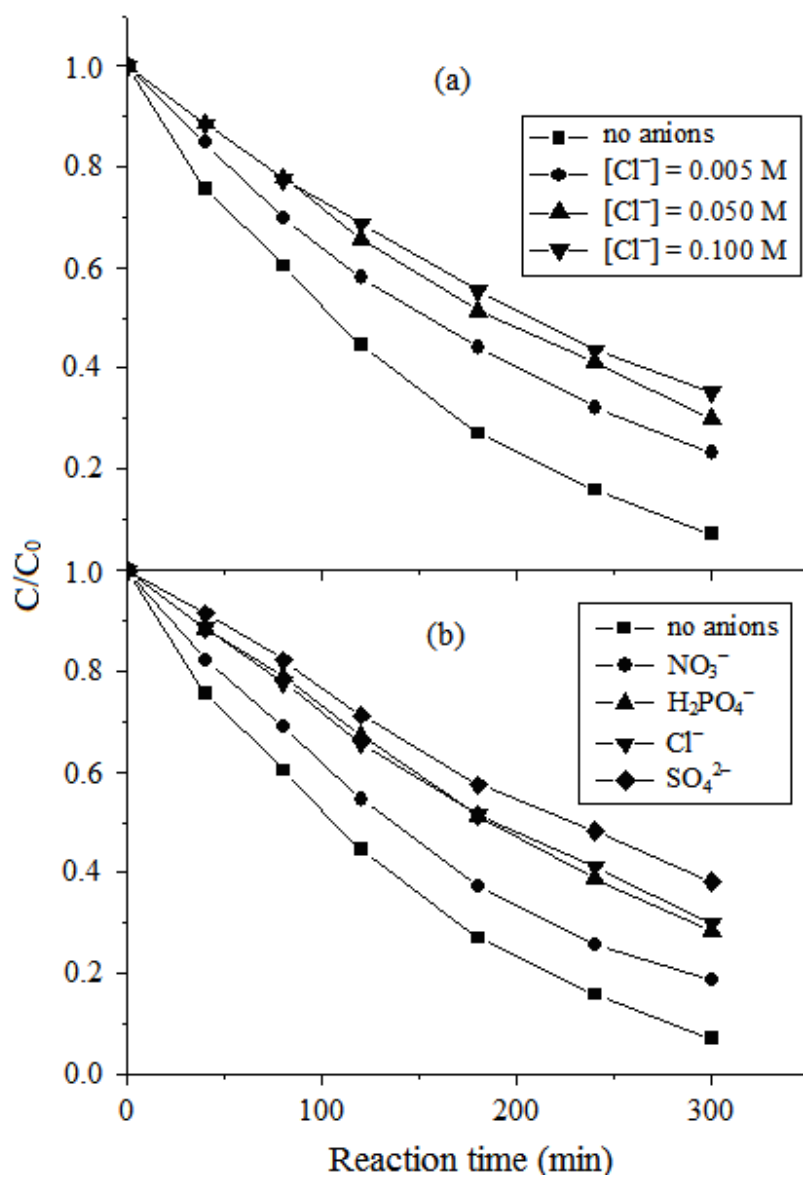
584

585

586 Fig. 5

587

588



589

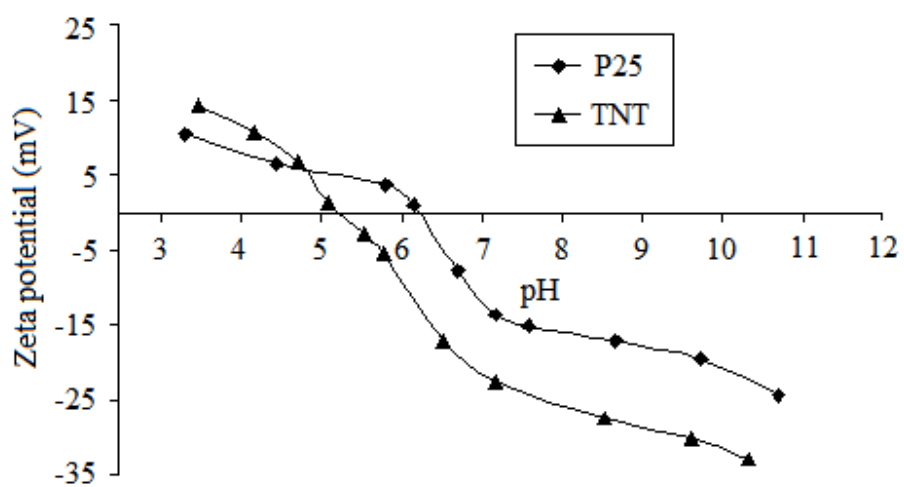
590

591

592

593

594 Fig. 6



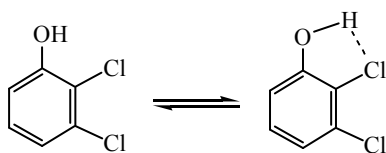
595  
596  
597  
598  
599  
600



601

602 Scheme 1.

603



604

605

606

607

608

609

610

611

612

613

614

615

616  
617  
618  
619  
620  
621  
622  
623  
624  
625  
626  
627  
628  
629  
630  
631  
632  
633  
634  
635  
636  
637  
638  
639  
640

Table 1

Effect of solution pH on the 2,3-DCP degradation, dechlorination, and DOC removal after 300 min reaction

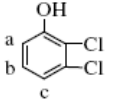
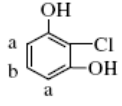
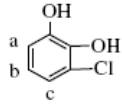
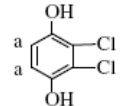
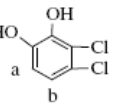
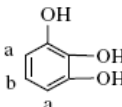
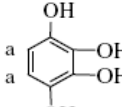
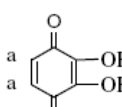
Test No.	pH		2,3-DCP degradation <sup>a</sup>		Dechlorination <sup>b</sup>	DOC reduction
	Initial	Final	$k$ (min <sup>-1</sup> )	(%)	(%, Cl <sup>-</sup> /Cl <sub>total</sub> )	(%)
1	3.4	3.0	0.007	90	52	47
2	5.3	3.4	0.008	93	57	40
3	7.8	3.8	0.011	96	74	37
4	10.9	7.1	0.024	100	99	20

<sup>a</sup> Photocatalytic degradation of 2,3-DCP was thought to be a pseudo-first-order reaction;  $k$  is the kinetic constant.

<sup>b</sup> Dechlorination was calculated on the basis of the total chlorine (Cl<sup>-</sup>/Cl<sub>total</sub>) in 2,3-DCP of 20 mg L<sup>-1</sup>.

641 Table 2

642 Identification of intermediates from 2,3-DCP degradation by <sup>1</sup>H-NMR analysis

Compound <sup>a</sup> No.	Proton	Chemical shifts (ppm)	Description <sup>b</sup>	Concentrations (mg L <sup>-1</sup> )		
				pH 3.4	pH 5.3	pH 10.9
	a	6.97	1H, d, $J_{ab} = 9.85$			
	b	7.18	1H, m,	47.2	47.2	26.0
	c	7.13	1H, d, $J_{cb} = 8.34$			
(2,3-dichlorophenol)						
	a	6.62	2H, d, $J_{ab} = 9.1$	12.6	18.9	90.1
	b	7.09	1H, t, $J_{ba} = 9.1$			
(2-chlororesorcinol)						
	a	6.52	1H, d, $J_{ab} = 8.9$			
	b	6.82	1H, m,	8.4	12.6	2.1
	c	6.86	1H, d, $J_{bc} = 8.9$			
(3-chlorocatechol)						
	a	6.75	1H, s	2.3	2.3	2.3
(2,3-dichloroquinol)						
	a	6.46	1H, d, $J_{ab} = 8.7$	trace	trace	6.9
	b	6.95	1H, d, $J_{ba} = 8.8$			
(5,6-dichlorocatechol)						
	a	6.40	2H, d, $J_{ab} = 8.3$	2.7	1.8	2.7
	b	6.61	1H, t, $J_{ba} = 8.1$			
(Pyrogallol)						
	a	6.08	2H, s	4.2	2.1	10.5
(1,2,3,4-benzenetetrol)						
	a	6.89	2H, s	1.7	1.7	1.6
(2,3-dihydroxy-p-benzoquinone)						

643

644 <sup>a</sup> Different protons linked on benzene ring are marked as a, b, and c, respectively.645 <sup>b</sup> Singlet, doublet, triplet, and multilet are abbreviated as s, d, t, and m, respectively; coupling646 constants ( $J$ ) are given hertz.